The immersed boundary method for two-dimensional foam with topological changes

Yongsam Kim[1,*], Yunchang Seol[1], Ming-Chih Lai[2], and Charles S. Peskin[3]

[1] *Department of Mathematics, Chung-Ang University, Dongjakgu Heukseokdong, Seoul 156-756, Korea.*
[2] *Department of Applied Mathematics, Institute of Mathematical Modeling and Scientific Computing, National Chiao Tung University, 1001, Ta Hsueh Road, Hsinchu 300, Taiwan.*
[3] *Courant Institute of Mathematical Sciences, New York University, 251 Mercer Street, New York, NY 10012 USA.*

Abstract. We extend the immersed boundary (IB) method to simulate the dynamics of a dry form, i.e., a foam in which most of the volume is attributed to its gas phase. In the article [Y. Kim, M.-C. Lai, and C. S. Peskin, J. Comput. Phys. 229:5194-5207, 2010], we implemented the IB method in the two-dimensional case, and tested it by verifying the von-Neumann relation which governs the coarsening of a two-dimensional dry foam. However, we had the principal limitation of the method used in that implementation: we do not allow for the resolution of quadruple or higher order junctions into triple junctions, which prevents a foam structure from completely coarsening. We here extend the methodology previously introduced and remove the limitation to study the coarsening process of a foam.

AMS subject classifications: 65-04, 65M06, 76D05, 76M20

Key words: foam, permeability, capillary-driven motion, immersed boundary method, coarsening, topological changes, T1 and T2 processes

1 Introduction

Liquid foams appear in daily life as the soap froth in a washing bowl or the head on a pint of bear. A foam is a gas-liquid mixture in which the volume of liquid is considerably smaller than that of the gas. Usually, in a "wet" foam (for which the volume of fraction of liquid is about 10%−20%), the bubbles are approximately spherical; while in a "dry" foam (for which the volume of fraction of liquid is less than 10%), the bubbles are more

*Corresponding author. *Email addresses:* enviho@gmail.com (Y. Seol),mclai@math.nctu.edu.tw (M.-C. Lai), peskin@cims.nyu.edu (C.S. Peskin),kimy@cau.ac.kr (Y. Kim)

nearly polyhedral in shape. One interesting phenomenon, which is called diffusive coarsening, is the evolution in bubble size and topological structure that occurs as a result of gas exchange between bubbles [11]. This gas exchange occurs by diffusion through the thin liquid boundaries that separate one bubble from another. The diffusive flux of gas through such a film is proportional to the pressure difference between the two bubbles that are separated by that boundary.

In [6], we have applied and extended the immersed boundary (IB) method to simulate the dynamics of a dry form in the two-dimensional case, and tested it by verifying the von-Neumann relation [8,9]: let A be the area of one bubble of a foam, then

$$\frac{dA}{dt} = -M\gamma \int_\Gamma \kappa dl = -2\pi M\gamma \left(1-\frac{n}{6}\right), \tag{1.1}$$

where M, γ, κ, and n are the permeability coefficient, surface tension, curvature of the bubble boundary Γ, and the number of vertices of the bubble, respectively. The von-Neumann relation simply says that the area is constant for 6-sided bubbles, that bubbles with fewer than 6 sides tend to disappear (and in fact reach zero area in finite time), and that bubbles with more than 6 sides tend to grow; hence the "coarsening" of the foam, in which bubbles with large numbers of sides grow at the expense of bubbles with small numbers of sides.

While we verified numerically the von-Neumann relation in [6], we showed the capability of the IB method to simulate the dynamics of a foam of an arbitrarily general shape which experiences the coarsening due to the gas diffusion through the foam boundaries. However, we had the principal limitation of the numerical method used in [6]: we do not allow for the resolution of quadruple or higher order junctions into triple junctions. Since a junction of more than 4 edges is unstable, after a short transient, it should change into triple junctions. Without the process of this resolution, the coarsening process comes to an end at some point without completing the coarsening of the whole foam structure, see Figure 11 in [6] for example.

We now extend the methodology introduced in [6] and remove the limitation to study the complete coarsening process of a foam. The extension is based on two primary topological processes which may occur in the evolution of a foam network [4, 11]. The first one, which is called T1 process, is needed when an edge of a bubble gradually shrinks and is about to make a quadruple junction. Since a quadruple junction is unstable, after some transient, this vertex decomposes to form two triple junctions, but in a different configuration. The second one, which is called T2 process, happens when a three-edged bubble gradually shrinks and finally disappear. Other topological changes are also possible through the combination of these two processes. For example, a four-sided bubble can disappear by a T1 process followed by a T2 process.

In addition to the topological changes, we generalize the initial configuration of a foam by using a Voronoi diagram [4, 11]. We choose randomly a set of points in a computational domain, and then construct the Delauney tessellation which divides the space into a set of triangles of which apices belong to the set of the initially chosen points.

A Voronoi network can be formed by convex hulls or cells whose boundaries are determined by all the perpendicular bisectors of the edges of the Delauney tessellation. Finally we relax the initial Voronoi network to obtain a more realistic shape of a foam in which the boundaries are curved and all the angles of the triple junctions are close to $2\pi/3$.

The rest of the paper is organized as follows. In Section 2, we describe the equations of motion of a foam. These are the typical IB equations of motion, generalized to handle a permeable boundary under surface tension. The numerical implementation is described in Section 3 which includes the way of performing the topological changes. The method to initialize a foam with a general configuration is presented in Section 4. In Section 5, we present simulation results which show the motion of the foams with 30 and 200 bubbles and the foam of a hexagonal structure with a minor defect. Some of the results are made as movie files and can be seen in the web 'http://cau.ac.kr/∼kimy'. Summary and conclusions are in Section 5.

2 Immersed boundary formulation

We summarize the equations of motion of the foam boundaries interacting with the surrounding gas which can diffuse through the foam boundaries. The equations of motion are as follows:

$$\rho(\frac{\partial \mathbf{u}}{\partial t}+\mathbf{u}\cdot\nabla\mathbf{u}) = -\nabla p+\mu\nabla^2\mathbf{u}+\mathbf{f}, \tag{2.1}$$

$$\nabla\cdot\mathbf{u} = 0, \tag{2.2}$$

$$\mathbf{f}(\mathbf{x},t) = \int \mathbf{F}(s,t)\delta(\mathbf{x}-\mathbf{X}(s,t))ds, \tag{2.3}$$

$$\begin{aligned}\frac{\partial \mathbf{X}}{\partial t}(s,t) &= \mathbf{u}(\mathbf{X}(s,t),t)+M\mathbf{F}/\left|\frac{\partial \mathbf{X}}{\partial s}\right|, \\ &= \int \mathbf{u}(\mathbf{x},t)\delta(\mathbf{x}-\mathbf{X}(s,t))d\mathbf{x}+M\mathbf{F}/\left|\frac{\partial \mathbf{X}}{\partial s}\right|,\end{aligned} \tag{2.4}$$

$$\mathbf{F}(s,t) = \frac{\partial}{\partial s}(\gamma\boldsymbol{\tau}), \tag{2.5}$$

$$\boldsymbol{\tau}(s,t) = \frac{\partial \mathbf{X}}{\partial s}/\left|\frac{\partial \mathbf{X}}{\partial s}\right|. \tag{2.6}$$

Eqs. (2.1)-(2.2) are the familiar Navier-Stokes equations for a viscous incompressible fluid. The unknown functions in the fluid equations are the fluid velocity, $\mathbf{u}(\mathbf{x},t)$; the fluid pressure, $p(\mathbf{x},t)$; and the force density applied by the immersed foam boundary to the fluid, $\mathbf{f}(\mathbf{x},t)$, where $\mathbf{x}=(x,y)$ are fixed Cartesian coordinates, and t is the time.

Eqs. (2.5)-(2.6) are the foam boundary equations which are written in Lagrangian form. The unknown $\mathbf{X}(s,t)$ completely describes the motion of the foam boundary and also its spatial configuration at any given time. The functions $\boldsymbol{\tau}(s,t)$ is the unit tangent

vector to the foam boundary, and the formula for $\mathbf{F}(s,t)$ is the standard one for a fiber under tension.

Eqs. (2.3) and (2.4) both involve the two-dimensional Dirac delta function $\delta(\mathbf{x}) = \delta(x)\delta(y)$, which expresses the local character of the interaction between the fluid and boundary. Eq. (2.3) simply expresses the relation between the two corresponding force densities $\mathbf{f}(\mathbf{x},t)d\mathbf{x}$ and $\mathbf{F}(s,t)ds$. Eq. (2.4) is the equation of motion of the immersed foam boundary in which M is the permeability constant. The second term both in second and third equations explains the normal flux through the foam boundaries (or normal slip of the boundaries relative to the fluid). This normal flux can be derived based on the two facts: (1) the formula for the normal equilibrium of the force density on the immersed boundary, and (2) the Darcy's law. For the detail of its derivation, see [6].

3 Numerical scheme

In this section we summarize the computational procedures used here and also in [6], and introduce the way to perform topological changes of the foam boundaries in the present simulation method.

3.1 Computational procedure

For the numerical implementation of the system Eqs. (2.1)-(2.6), we use a standard first-order IB method, generalized to take a permeable foam boundary into account [5, 6]. In this method, we update the data given at time level n to obtain those at time level $n+1$ using the forward Euler's method. The step-by-step procedure of the numerical implementation used here and in [6] can be summarized as follows:

Step 1: Using the position of the internal boundary foam $\mathbf{X}^n$, calculate the Lagrangian force density by

$$\mathbf{F}_k^n = \frac{\gamma}{\Delta s}\sum_{i=1}^{n_f-1}\frac{\mathbf{X}_{i+1}^n-\mathbf{X}_i^n}{|\mathbf{X}_{i+1}^n-\mathbf{X}_i^n|}(\delta_{i,k}-\delta_{i,k-1}), \tag{3.1}$$

where $\delta_{i,k}$ is the Kronecker symbol which is 1 when $i=k$ and 0 otherwise. This force density is derived from the relation $\mathbf{F}_k^n\Delta s = -\partial E/\partial \mathbf{X}_k^n$, where $E[\mathbf{X}^n]$ is the discretized energy functional of the form $E[\mathbf{X}^n] = \gamma\sum_{k=1}^{n_f-1}|\mathbf{X}_{k+1}^n-\mathbf{X}_k^n|$.

Step 2: Distribute this tension force defined on Lagrangian grid points into the force at Eulerian spatial grid points to be applied in the Navier-Stokes equations. This is done by a discretization of Eq. (2.3) as

$$\mathbf{f}^n(\mathbf{x}) = \sum_k \mathbf{F}_k^n\delta_h(\mathbf{x}-\mathbf{X}_k^n)\Delta s, \tag{3.2}$$

where $\mathbf{x} = (x_1,x_2)$ is the fluid mesh point, and δ_h is the smooth version of Dirac delta function [10].

Step 3: Given the Eulerian force density $\mathbf{f}^n(\mathbf{x})$, we are ready to solve the descritized version of the fluid equations Eqs. (2.1)-(2.2). In the present work, we employ a typical solver for the incompressible Navier-Stokes equations which uses a staggered-grid discretization (MAC scheme) for the spatial direction and the forward Euler's method for the temporal direction [1,2].

Step 4: Update the foam boundary points which are moved at the local fluid velocity of the updated velocity field, corrected by the relative slip. This is done by approximating Eq. (2.4) as follows:

$$\frac{\mathbf{X}_k^{n+1}-\mathbf{X}_k^n}{\Delta t}=\sum_{\mathbf{x}}\mathbf{u}^{n+1}(\mathbf{x})\delta_h(\mathbf{x}-\mathbf{X}_k^n)h^2+\frac{M\mathbf{F}_k^n\Delta s}{(|\mathbf{X}_{k+1}^n-\mathbf{X}_k^n|+|\mathbf{X}_k^n-\mathbf{X}_{k-1}^n|)/2}. \tag{3.3}$$

We assume, however, that there is no permeability at the junctions where three (or more) internal boundaries meet. These junctions simply move at the local fluid velocity, that is, by Eq. (3.3) with $M=0$.

Note that, at the end of each iteration, we redistribute the internal boundary points $\mathbf{X}_k^n$ of the foam to maintain reasonable resolution along the boundary. A proper resolution of the boundary is maintained by the two processes: (1) adding a new immersed boundary point when the distance between neighboring boundary points $|\mathbf{X}_{k+1}^n-\mathbf{X}_k^n|>h/2$, or (2) deleting both points and creating in their place a new boundary point halfway between them when $|\mathbf{X}_{k+1}^n-\mathbf{X}_k^n|<h/4$. In addition to the redistribution of the internal boundary points, we perform topological changes when they are needed in each iteration. We now explain how we deal with them.

3.2 Topological changes

Topological changes are needed to resolve quadruple or higher order junctions into triple junctions. Since a junction of more than 4 edges is unstable, after a short transient, it should change into a triple junction. Moreover the coarsening process cannot complete without the resolution process [6]. The topological changes of a foam are composed of the two primary topological processes which may occur in the evolution of a foam network [4,11]: (1) the switch of a side of the foam boundaries ('T1' process), and (2) the removal of a three-sided bubble ('T2' process). Other topological changes are also possible through the combinations of these two processes. For example, a four-sided bubble can disappear by a T1 process followed by a T2 process.

The T1 process is needed when an edge of a bubble gradually shrinks and is about to make a quadruple junction. Since a quadruple junction is unstable, after some transient, this vertex decomposes to foam two triple junctions, but in a different configuration, see Figure 1. The effect of T1 process is to reduce by one the number of edges of two cells, and to increase by one the number of edges of two other cells.

In order to realize the T1 process, we count the number of internal boundary points on each bubble edge at each iteration. We declare that the edge is a candidate for switching when and only when there are no interior points on the edge, i.e., when the two vertices

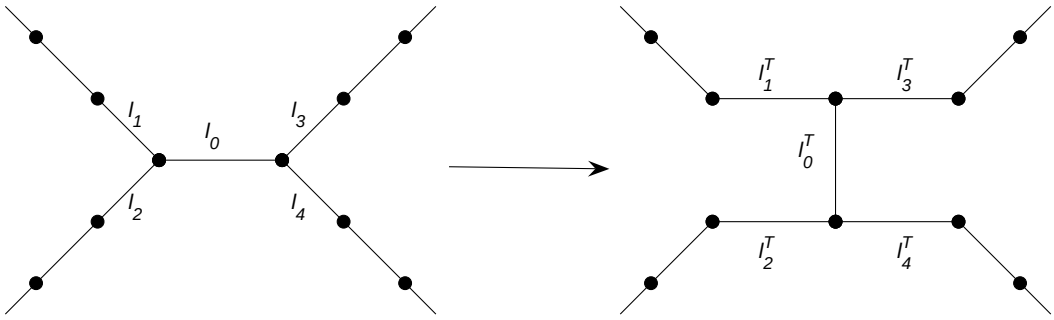

Figure 1: T1 process: the bubble edge on which there is no interior marker points is a candidate for switching (left). We rotate the edge by 90 degrees about its center, break the old connections, and make the new ones (right). This switch, however, is actually made only when $\sum_{i=1}^{4} l_i \geq \sum_{i=1}^{4} l_i^T$, which lowers the potential energy.

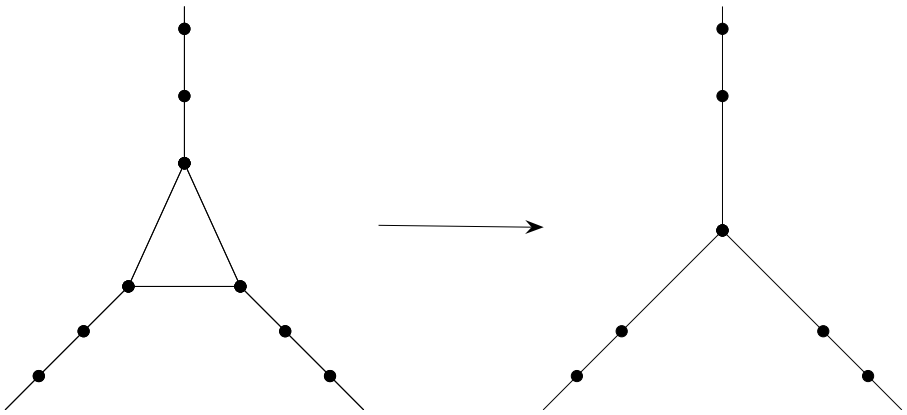

Figure 2: T2 process: whenever there are no interior points on the edges of a three-edged bubble (left), we replace the three-edged bubble by one vertex at the center of the bubble, and connect the new vertex directly to the three edges which previously formed triple junctions with the three-edged bubble (right).

of the edge are connected directly to each other, see the left plot of Figure 1. When two vertices on an edge are candidates for switching, we try the switch but actually make it only if it lowers the total energy (i.e., length) of the boundary. The meaning of "try the switch" is to rotate the edge by 90 degrees about its center, to break the old connections, and to make the new ones by connecting the rotated edge to the other four edges which previously formed the two triple junctions, see the right plot of Figure 1. Since this switch involves breaking four links and creating four new ones, it is only the lengths of these links l_i and l_i^T, i=1, 2, 3, 4 that need to be considered in deciding whether to make the switch. The actual switch is made only when $\sum_{i=1}^{4} l_i \geq \sum_{i=1}^{4} l_i^T$. Note that, by definition, we make a switch only when it lowers the potential energy.

The T2 process is the disappearance of a three-edged bubble when three vertices of the bubble become one point (vertex). Whenever all the edges of a three-edged bubble have no interior points and are connected directly to each other as shown in the left plot

of Figure 2, we replace the three-edged bubble by one vertex at the center of the bubble, and connect the new vertex directly to the three edges which previously formed triple junctions with the three-edged bubble, see the right plot of 2. As in the T1 process, the T2 process does slightly change the potential energy of the boundary, but only by lowering it. Thus, the T1 and T2 processes may be viewed as a kind of numerical dissipation of energy, and this loss of energy is part of the numerical error of the scheme.

4 Initial configurations

Consider the incompressible viscous fluid in a square box $[0,1]\times[0,1]$ with periodic boundary conditions which contains a network of foam boundaries. We construct a Voronoi diagram to set up an initial configuration of a foam [4], see Figure 3. To do that, we first choose randomly a set of points in a box $[0,1]\times[0,1]$ which shall sit inside each bubble of a foam. In order to take the periodicity into account, we extend the unit square box into a square $[-1,2]\times[-1,2]$ and copy the set of points chosen in $[0,1]\times[0,1]$ periodically into $[-1,2]\times[-1,2]$. Next, we construct the Delauney tessellation which divides the space into a set of triangles of which apices belong to the set of the chosen points in $[-1,2]\times[-1,2]$. With the dual relationship between Delauney triangulation and Voronoi diagram, a Voronoi network can be formed by convex hulls or cells of which the boundaries are determined by all the perpendicular bisectors of the edges of the Delauney tessellation. Now we consider only the square box $[0,1]\times[0,1]$ as the computational domain in which a network of foam boundaries exists periodically, see Figure 3.

Since the Voronoi network as an initial configuration of a foam is composed of a set of straight lines, we relax the initial foam network to obtain a more realistic shape of a foam in which the boundaries are curved and all the angles of the triple junctions are close to $2\pi/3$. To do that, we apply to the given Voronoi network the present IB computation with zero permeability until the pressure change in time is small. Since the permeability of the foam is 0 and there is no diffusion of the gas through the foam boundaries, each bubble of the foam changes its shape but does not change its area. Figure 4 shows a 'relaxed' configuration of the foam (left) obtained from the Voronoi network shown in Figure 3 and the corresponding pressure contours (right). The dashed line in the left figure represents the periodic unit square. Note that the bold lines in the pressure contours are mainly near the internal foam boundaries indicating that the biggest pressure differences are across the boundaries.

5 Results and Discussion

In this section, we show the simulation results obtained by the numerical scheme presented in Section 3. The foams have general configurations and go through the topology changes based on T1 and T2 processes. Some of the results are made as movie files which can be seen in the web 'http://cau.ac.kr/∼kimy'.

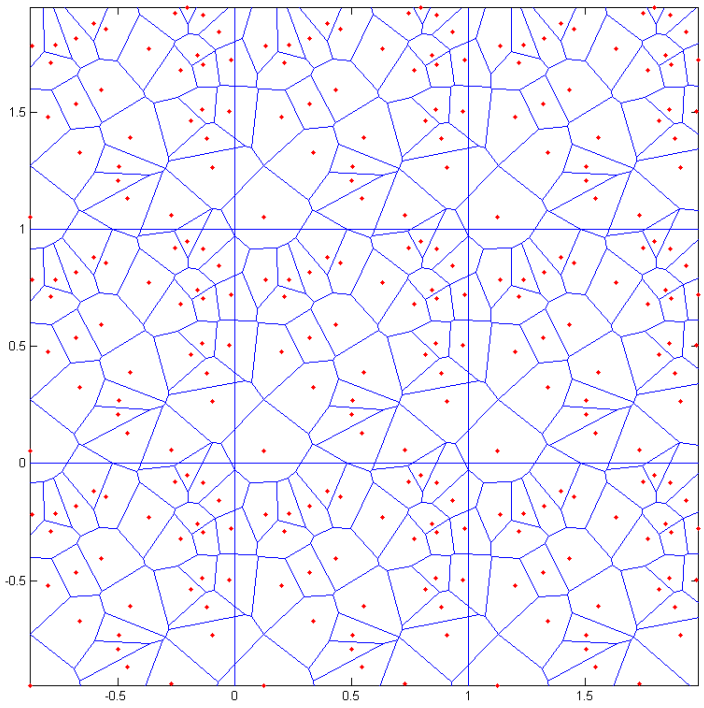

Figure 3: A set of points (30 dots) is randomly chosen in a square $[0,1]\times[0,1]$ and copied periodically into $[-1,2]\times[-1,2]$. A Voronoi network is constructed to be an initial configuration of a foam. The square box $[0,1]\times[0,1]$ is the computational domain in which a network of foam boundaries exists periodically.

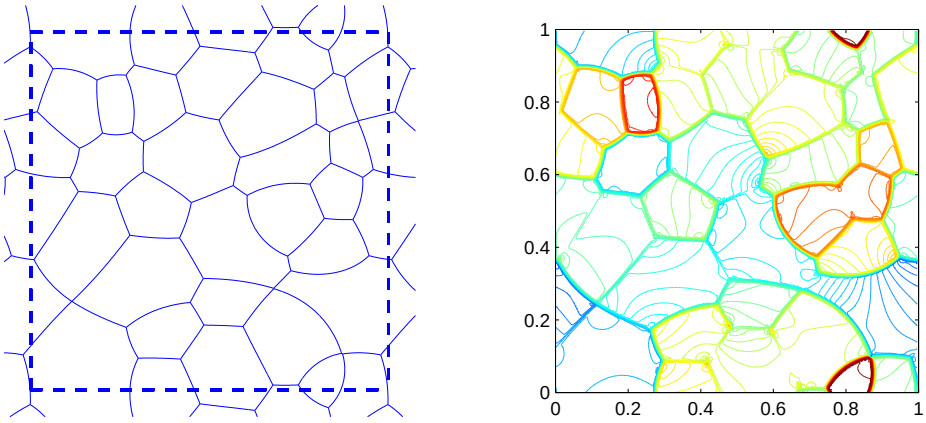

Figure 4: Initial configuration: the 'relaxed' configuration of a foam (left) obtained from the Voronoi network shown in Figure 3 and the corresponding pressure contours (right). The dashed line in the left panel represents the periodic unit square.

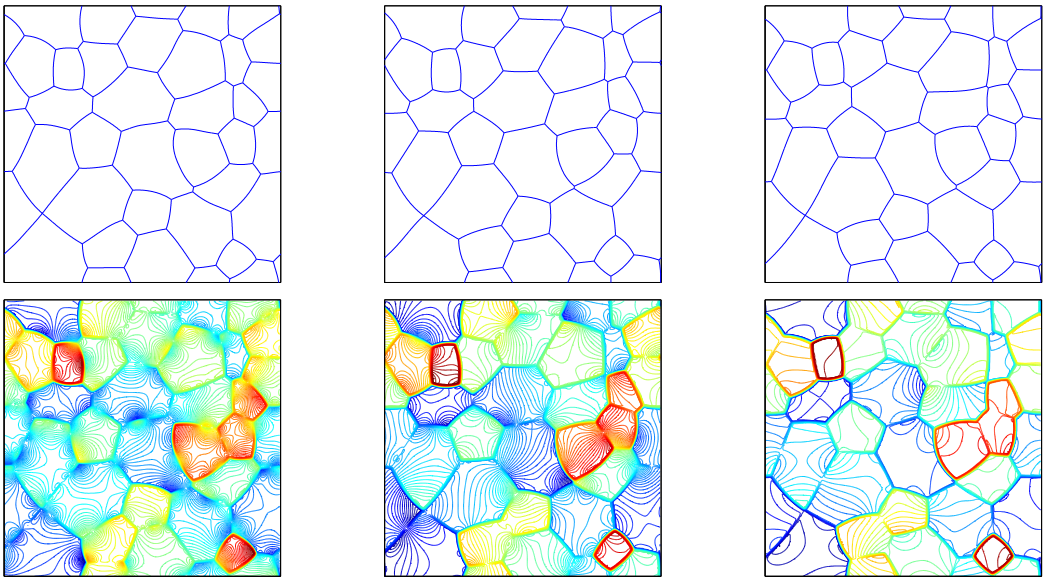

Figure 5: The configurations of the foam (upper panels) and the pressure contours (lower panels) at some selected times: $t=0.3$ (left), $t=0.6$ (middle), and $t=0.9$ (right). Since the permeability M is zero, the foam moves only slightly.

Throughout this paper, we choose the computational domain $\Omega=[0,1]\times[0,1]$ with the periodic boundary conditions, and use the mesh width $h=\Delta x=\Delta y=1/256$, which is uniform and fixed in time, and the time step duration $\Delta t=10^{-5}$. The fluid density is chosen as $\rho=1$, the viscosity $\mu=0.001$, and the surface tension coefficient $\gamma=2$. Note that these parameters are arbitrarily chosen and do not correspond to any particular physical case. We use two different permeabilities, M=0 and 0.04 to see how the permeability affects the foam dynamics.

As the first case, we start with the foam shown in Figure 4 which has 30 bubbles. We choose the permeability M to be 0. Figure 5 shows the configurations of the foam (upper panels) and the pressure contours (lower panels) at some selected times: $t=0.3$ (left), $t=0.6$ (middle), and $t=0.9$ (right). Since the permeability is zero and the fluid is incompressible, the foam moves only slightly. Note that the pressure contours enable us to recognize the configurations of the foam without even drawing them, see the lower panels. The colors in the pressure contours are mainly near the internal foam boundaries, and each such boundary has a reddish color on one side, and a bluish color on the other, thus indicating that the biggest pressure differences are across the foam boundaries, as they should be.

When the permeability M is 0.04, Figure 6 shows the motion of the foam (upper panels) and the pressure contours (lower panels) at some selected times: $t=0.15$, $t=0.3$, $t=0.45$, $t=0.6$, $t=0.75$, and $t=0.9$. In this case, the gas exchange occurs by diffusion through the foam boundaries that separate one bubble from another. By the diffusive

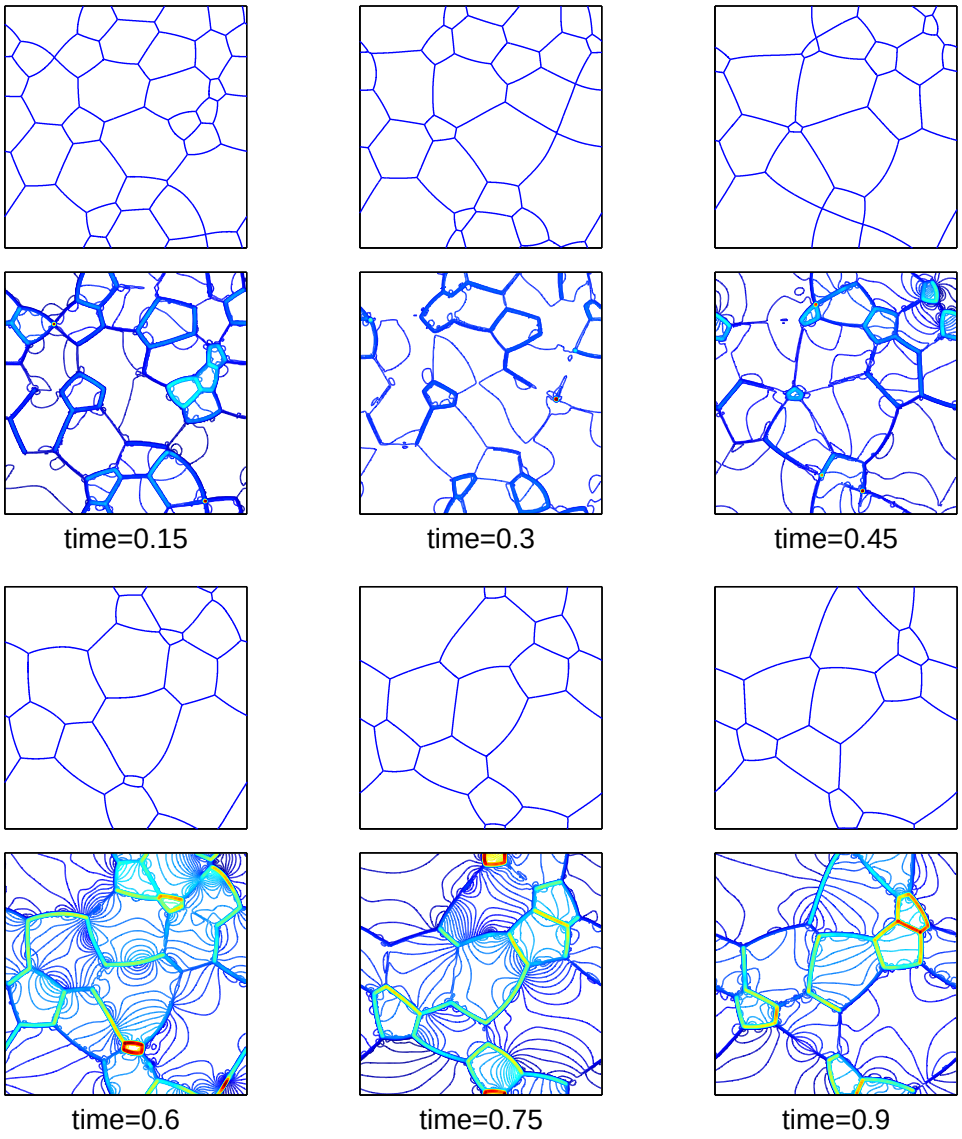

Figure 6: The motions of the foam (upper panels) and the pressure contours (lower panels) at the selected times: $t=0.15$, $t=0.3$, $t=0.45$, $t=0.6$, $t=0.75$, and $t=0.9$. The permeability M is 0.04. We can observe the diffusive coarsening with topological changes.

coarsening, the bubbles evolve changing their sizes and sometimes go through the topological changes based on T1 and T2 processes explained the above, especially, compare the figures at $t = 0.15$ and $t = 0.9$. We can also recognize the configurations of the foam from the pressure contours in the lower panels. Since the motion of the fluid is quite dynamic, the pressure is not a constant within each bubble, for the gradients in the pressure are what produces the fluid accelerations.

If all the bubbles in a foam has a hexagonal shape, since they have 6 edges, the foam does not experience topological changes and approaches quickly the state of an equilibrium in which all the angles of the triple junctions are $2\pi/3$ degrees. However, if the foam of a hexagonal structure has a minor defect, then the defect spreads due to the diffusive coarsening as shown in Figure 7. Here the defect is set up by first choosing an hexagonal structure and then by modifying the foam to have 5-edged and 7-edged bubbles, see the first panel in Figure 7. The spreading of a defect shown in 7 is comparable to Fig. 7.8 in [11].

Finally we simulate the coarsening process of a foam with 200 bubbles immersed in the domain $\Omega = [0,1] \times [0,1]$. Since the computational time of our method is mostly consumed in solving the fluid equations, the total computational cost is dependent only slightly on the number of bubbles. Figures 8 and 9 show the motions of the foam (upper panels) and the pressure contours (lower panels) at some chosen times. At early times shown in Figure 8, the foam goes through fast topological changes based on T1 and T2 processes, but, at later times shown in Figure 9, its topological changes slow down. Notice the different time scales between Figs. 8 and 9.

6 Summary and Conclusions

We have used an immersed boundary method to simulate the fluid dynamics of a two-dimensional dry foam and have extended the model to allow for the topological changes of the foam network. These topological changes are based on T1 and T2 processes and enable a foam to complete the total coarsening. Future work includes the extension of the methodology introduced here to the study of three-dimensional foams [3,7].

Acknowledgement The first author was supported by National Research Foundation of Korea Grant funded by the Korean Government (2010-0016611).

References

[1] B.E. Griffith and C.S. Peskin, *An accurate and efficient method for the incompressible Navier-Stokes equations using the projection method as a preconditioner.* J. Comput. Phys. 228:7565-7595, 2009.

[2] F.H. Harlow and J.E. Welch, *Numerical calculation of time-dependent viscous incompresible flow of fluid with free surface.* Phys. Fluid. 8(12):2182-2189, 1965.

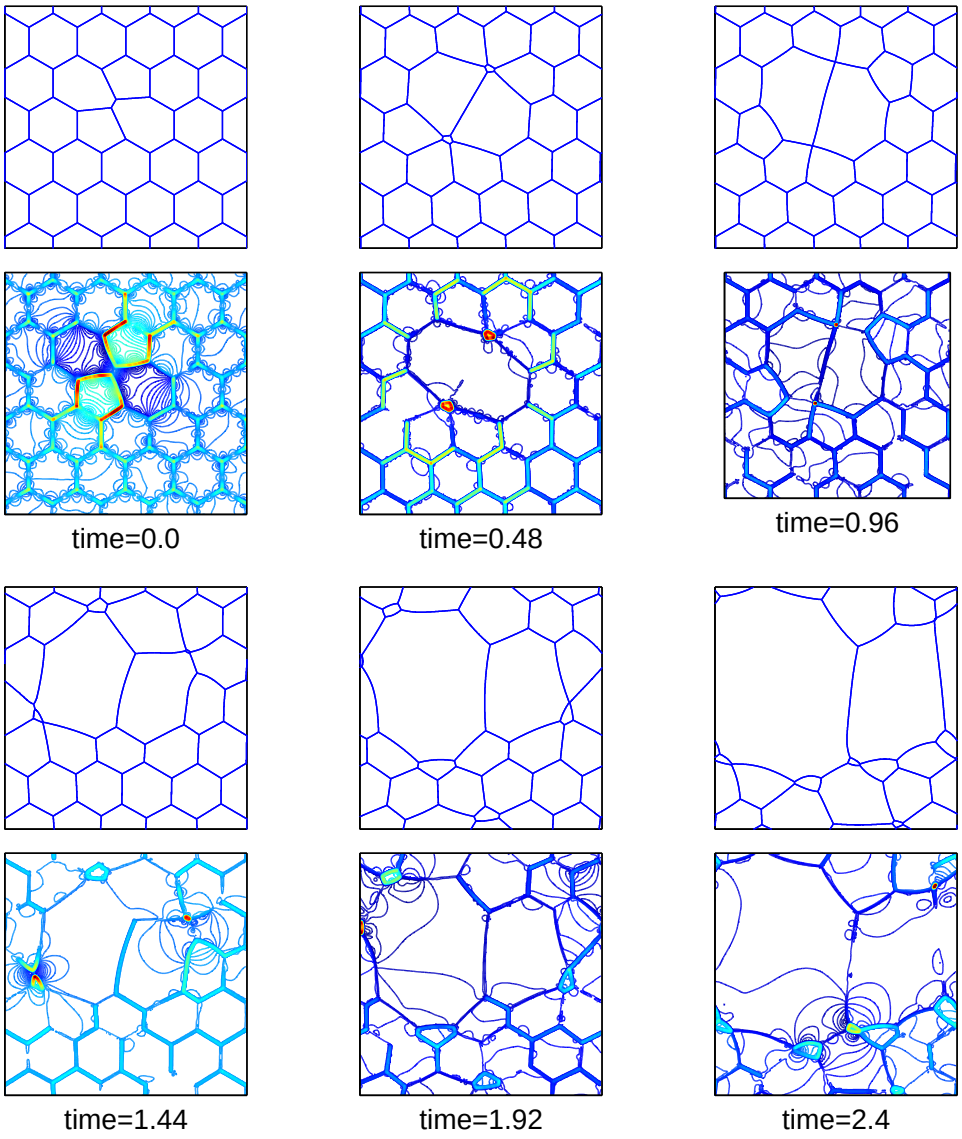

Figure 7: Spreading of a defect in a hexagonal structure due to the diffusive coarsening with topological changes. The motion of the foam (upper panels) and the pressure contours (lower panels) are drawn at the selected times: $t=0.0$, $t=0.48$, $t=0.96$, $t=1.44$, $t=1.92$, and $t=2.4$.

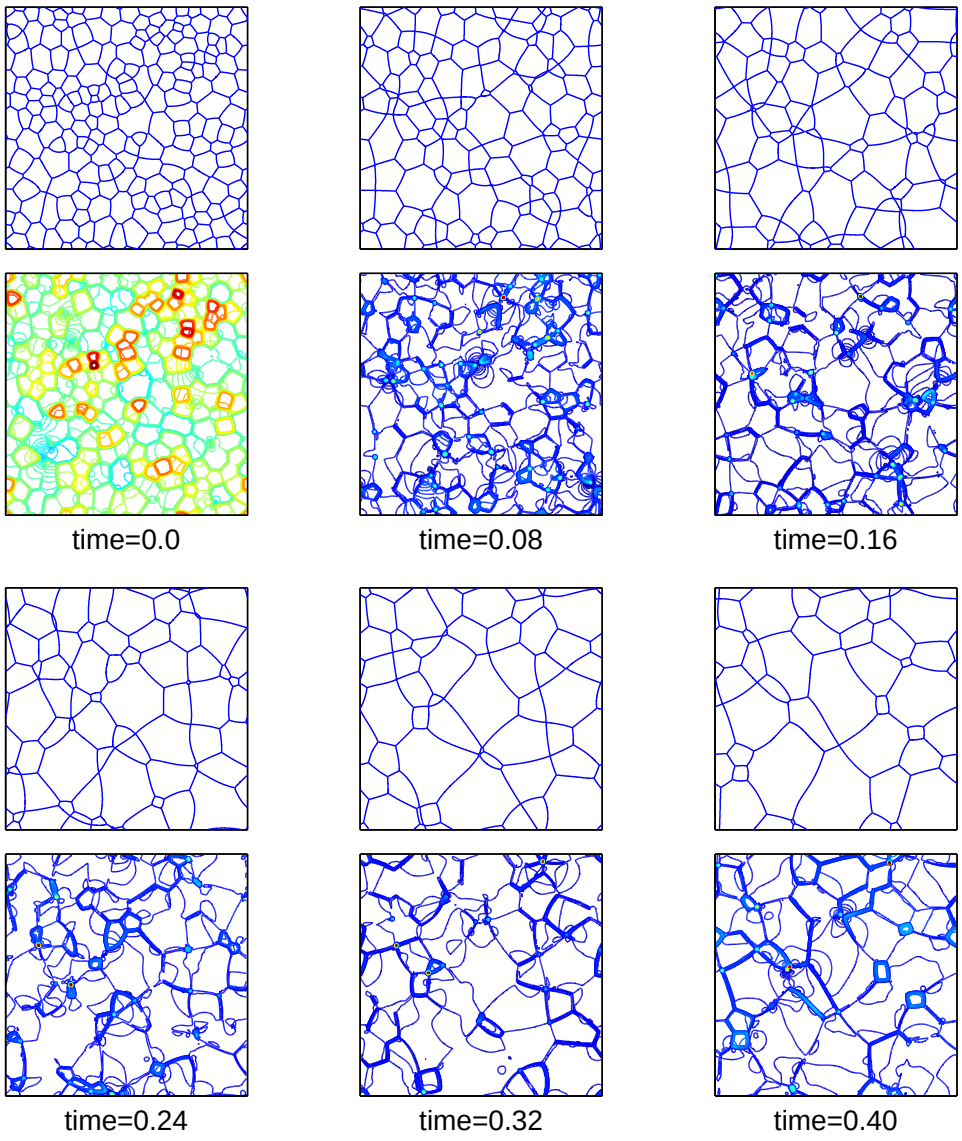

Figure 8: The configurations of the foam (upper panels) and the pressure contours (lower panels) at early times. The number of bubbles is 200 and the permeability is M=0.04.

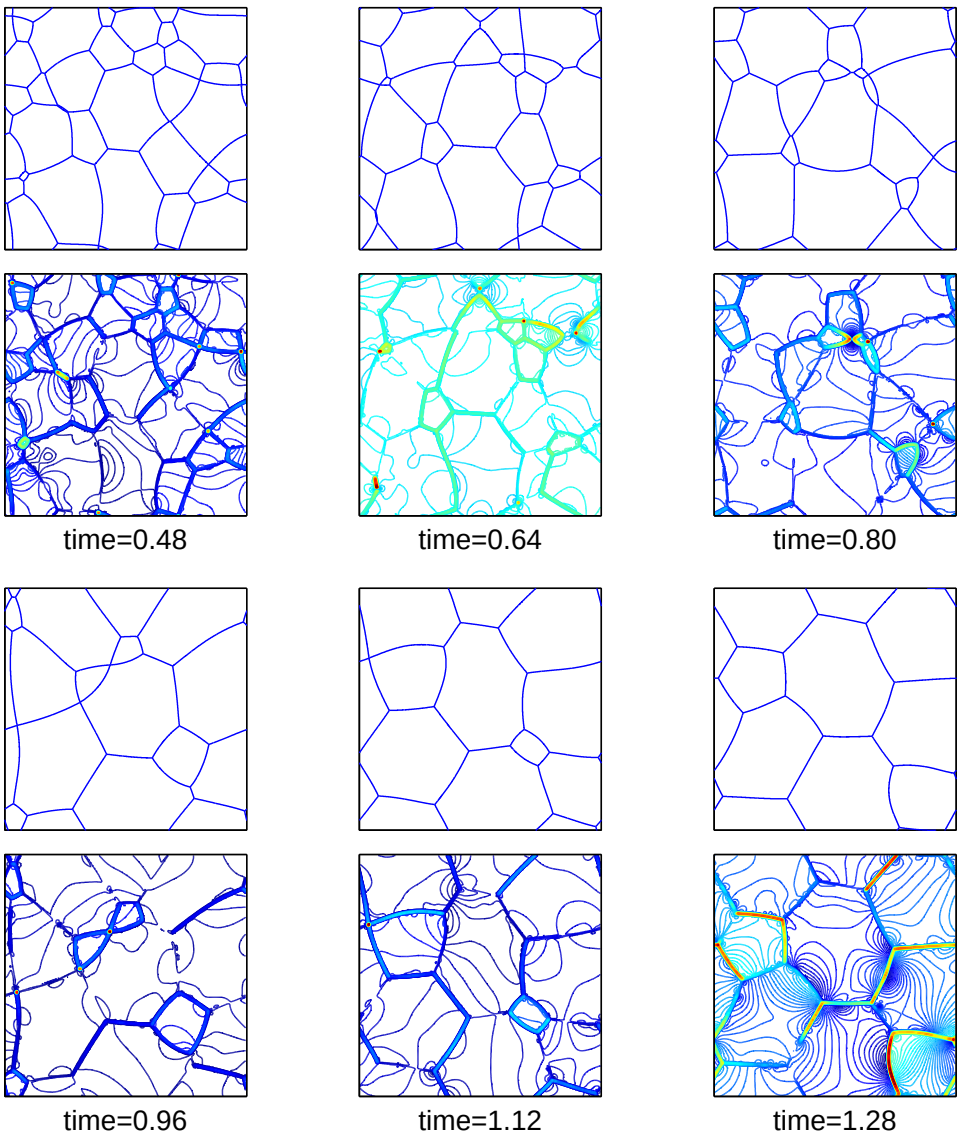

Figure 9: The same as Figure 8 at later times. The time scale here is larger than that in Figure 8.

[3] S. Hilgenfeldt, A.M. Kraynik, S.A. Koehler, and H.A. Stone, *An accurate von Neumann's law for three-dimensional foams*, Phys. Rev. Lett. 86(12):2685-2688, 2001.
[4] J.P. Kermode and D. Weaire, *2D-Froth: a program for the investigation of 2-dimensional froths.* Computer Physics Communications 60, 75-109, 1990.
[5] Y. Kim and C.S. Peskin. *2-D parachute simulation by the Immersed Boundary Method.* SIAM J.Sci.Comput. 28(6), 2006.
[6] Y. Kim, M.-C. Lai, and C.S. Peskin, *Numerical simulations of two-dimensional foam by the immersed boundary method.* J. Comput. Phys. 229:5194-5207, 2010.
[7] R.D. MacPherson and D.J. Srolovitz, *The von Neumann relation generalized to coarsening of three-dimensional microstructures,* Nature, 446(26):1053-1055, 2007.
[8] W.W. Mullins, *in Metal Surfaces: Structure, Energetics, and Kinetics.* (eds. W.D.Robertson and N.A.Gjostein) 17-66(American Society for Metals, Metals Park, Ohio, 1963).
[9] von Neumann, J. in Metal Interfaces (ed. C.Herring) 108-110(American Society for Metals, Cleveland, 1951).
[10] C.S.Peskin, *The immersed boundary method* Acta Numerica, 11:479-517, 2002.
[11] D. Weaire and S. Hutzler, *The Physics of Foams*, Oxford University Press, 1999.